Available online at www.sciencedirect.com
SCIENCE DIRECT®
Journal of Chromatography A, 1074 (2005) 53–59
JOURNAL OF CHROMATOGRAPHY A
www.elsevier.com/locate/chroma

Estimation of diffusion parameters in functionalized silicas with modulated porosity Part I: Chromatographic studies

G.S. Armatas, D.E. Petrakis, P.J. Pomonis *

Department of Chemistry, University of Ioannina, Dourouti, Ioannina 45 110, Greece

Received 14 September 2004; received in revised form 7 March 2005; accepted 10 March 2005
Available online 2 April 2005

Abstract

The diffusion parameters of binary gas mixture He (tracer gas)–N_2 (carrier gas) in hybrid organic–inorganic SiO_2-X porous solids which have suffered gradual functionalization with functional groups X of increasing length (X = ∅, ≡Si–H, ≡Si–CH_2OH, ≡Si–$(CH_2)_3$OH, ≡Si–$(CH_2)_{11}CH_3$) are reported. The effective diffusivities D_{eff}, the Henry law constants K as well as the tortuosity factors τ for the examined solids were estimated by a typical pulse gas chromatographic method. Analysis of the experimental results was carried out by the well-known method of linearization of moments. The moments s analysis provides a powerful means for extracting diffusion parameters from the experimental response curves The proposed methodology is simple compared to other similar studies and provides rapidly reliable data. The results of this work indicate that the effective diffusivity D_{eff} in porous networks drops markedly as the initial porosity of the parent SiO_2 sample is blocked by the functionalization of the pore surfaces with functional groups of increasing size, ≡Si–H, ≡Si–CH_2OH, ≡Si–$(CH_2)_3$OH and ≡Si–$(CH_2)_{11}CH_3$. The low values of the Henry law constants K found indicate that the adsorption of He on the porous surfaces for all the solids is weak. Also, the tortuosity factor τ is proportionally correlated to the pore blocking effects and the percolation phenomena of gases flowing into the porous network.

Keywords: Effective diffusivity; Tortuosity factors; Henry constants; Porous solids; Functionalized silica; Gas chromatography

1. Introduction

It is often very useful to characterize the mass transfer inside various porous catalysts and adsorbents in terms of an *effective diffusivity*. Unfortunately, it is not possible to obtain effective diffusivities by simply correcting bulk phase diffusivities by the reduction of the cross-section area due to the porous solid phase. The more important reasons render this simple approach invalid are: (i) interconnections within the pore structure, the tortuous character of individual pores and variations in cross-section area along the pore length contribute to the difficulty of the task, and (ii) one or more of several different mechanisms may be responsible for the mass transfer process. These include bulk diffusion, Knudsen diffusion and surface diffusion. For the majority of the catalysts and conditions used in industrial practice, the only significant mechanisms are bulk diffusion and Knudsen diffusion. The surface diffusion is taken into consideration only when adsorption is important.

The diffusion parameters can be estimated from theoretical calculations by using suitable mathematical diffusion models. In such cases, a model of the pore network is required that simulates satisfactorily the pore structure. Then in that model the suitable equations of diffusion can be applied. The choice of the model influences considerably the result and affects the reliability of results. Thus, the experimental determination of diffusion parameters in porous materials requires precise measurements and usually complex mathematical analysis of the results.

A large number of techniques have been employed to measure the effective diffusivity in porous solids [1,2]. Among these the gas chromatography has emerged as a practical and popular tool for evaluating effective diffusivities. The prin-

* Corresponding author. Tel.: +32 651098350; fax: +32 651098795.
E-mail address: ppomonis@cc.uoi.gr (P.J. Pomonis).

0021-9673/$ – see front matter © 2005 Elsevier B.V. All rights reserved.
doi:10.1016/j.chroma.2005.03.046

cipal advantage of this method is that measurements can be easily conducted at elevated temperatures and pressures. In the literature, different methodologies have been proposed which take into account the influence of pressure drop at the ends of column [4,5], the thermal diffusion resistance [6], the peak broadening from axial dispersion [7] and the dispersion of pulse injection of the tracer [8].

Among the methods of analysis which have been employed, the most popular ones are methods based on the moments of the response curve. The moments s analysis provides a powerful means for extracting diffusion parameters from the experimental response curves. Thus, the models of the Kubin [9], Kucera [10] and Suzuki-Smith [11], relate the moments to the transport parameters of the processes taking place in a column packed with porous particles. The major advantage of those methodologies is their simplicity. Besides the large number of measurements, which can be easily conducted at different velocities, can be correlated in order to provide meaningful data about the diffusion parameters. Nevertheless, efforts to distinguish between the various modes, i.e. axial dispersion, intraparticle resistance and external resistance of the mass transport resistances have not proven easy [12]. Thus, several investigators have proposed modifications of the pulse chromatography experiments with the purpose of reducing the relative contribution of axial dispersion to the mass transport processes [4,13]. Usually, the moments method would be used to fit the experimental response curves as a function of time. In such cases an appropriate objective function is defined and the model parameters are obtained by optimization to experimental data [14–16]. However, the approach is complicated by the fact that numerical means with complex algebric solutions are needed, which sometimes can be tedious.

In Part I of this work, we report the diffusion parameters of binary gas mixture He (tracer gas)–N_2 (carrier gas) in hybrid organic–inorganic SiO_2-X porous solids which suffered gradual functionalization with functional groups X of increasing length (X = Ø, ≡Si–H, ≡Si–CH_2OH, ≡Si–$(CH_2)_3$OH, ≡Si–$(CH_2)_{11}CH_3$). The effective diffusivities D_{eff}, the Henry law constants K as well as the tortuosity factors τ for the examined solids were estimated by pulse gas chromatography method. Analysis of the experimental results was carried out by the simple method of linearization. The proposed methodology is simple compared to previous similar studies [3,7] and provides rapid and reliable results. In Part II, we propose a model for the porous network of the above materials and compare the corresponding results.

2. Experimental

2.1. Synthesis of materials

The inorganic support SiO_2 was synthesized as follows: commercial tetraethoxysilane (TEOS, Aldrich), oxalic acid (OA, Aldrich) and hexanol (Fluka) were used without purification. An amount of OA in 0.66 mol hexanol was mixed with 0.40 mol of TEOS in ratio OA:4TEOS = 7.5 in a 500 ml two-necked flask. The reaction mixture was kept at 70 °C for 2 h under mechanical stirring. Then, 4.0 moles of deionized water (H_2O/TEOS molar ration = 10) were added. After 24 h at 70 °C under mechanical stirring the resulting solid was recovered by filtration, washed with ethanol and distilled water and dried in air at 100 °C for 12 h. The organic part was removed by calcination at 873 K for 6 h.

Four samples, based of the original porous solid SiO_2, were prepared with gradual functionalization of its acid sites with a organo-silicate groups (X = ≡Si–H, ≡Si–CH_2OH, ≡Si–$(CH_2)_3$OH, ≡Si–$(CH_2)_{11}CH_3$). The functionalization was carry out as follows: The inorganic support SiO_2 (X = Ø) was dried in an oven at 150 °C for 2 h and refluxed in toluene for 12 h with the estimated amount of the corresponding organic alkoxy silanes $(CH_3O)_3$≡Si–H (trimethoxy-silane, Aldrich), $(CH_3CH_2O)_3$≡Si–CH_2Cl (chloro-methyl-triethoxy silane, Fluka), $(CH_3O)_3$≡Si–$(CH_2)_3$Cl (chloro-propyl-trimethoxy silane, Aldrich) and $(CH_3CH_2O)_3$≡Si–$(CH_2)_{11}CH_3$ (dodecyl-triethoxy silane, Fluka) with carbon chain of different length. The resulting solids were recovered by filtration, washed with toluene and ethanol and dried in air at 110 °C for 24 h. Further details about these solids are in a recent publication [17]. We also mention that the approximate bonding density of the functional groups was about 1 group per 100–120 Å, similar to that of the surface density of the acid sites determined by titration with NH_3 (NH_3 temperature programmed desorption).

2.2. N_2 porosimetry

A Fisons Sorptomatic 1900 instrument was used to carry out the pore size distribution measurements for the five SiO_2-X materials. The characterization included the determination of nitrogen adsorption–desorption isotherms at 77 K. Prior to each experiment the samples were degassed at 60 °C in a vacuum of 5×10^{-2} mbar for 24 h for the SiO_2-X. The desorption branch of the isotherms was used for the calculation of the pore size distribution PSD. The specific surface area of the sample was calculated by applying the BET equation using the linear part ($0.05 < P/P_0 < 0.25$–0.30) of adsorption isotherm and assuming a closely packed BET monolayer.

2.3. Chromatographic apparatus and procedure

A schematic diagram of the experimental arrangement is shown in Fig. 1. The apparatus consist of the carrier gas (N_2) and the tracer gas (He), a small column which contains the well packed sample, a gas chromatograph type Shimadzu GC-8A, equipped with a thermal conductivity detector (TCD) and a suitable computer system for the recording of data. The packing of the column took place by sieving the sample and using the fraction 1.25×10^{-2} cm < R of the particles. The inside diameter of the column was 2 mm and its length 11 cm. The column was mounted in the gas chromatograph

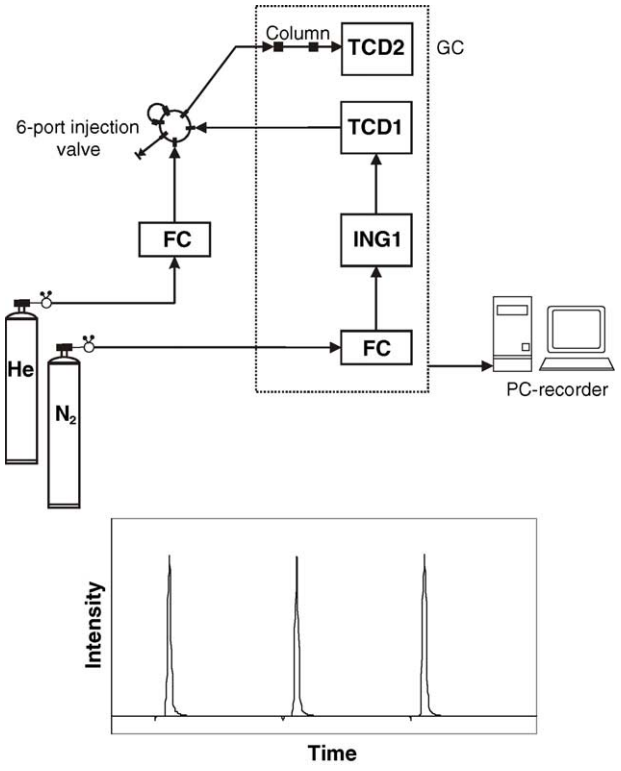

Fig. 1. Upper part: experimental apparatus for the pulse gas chromatographic method (CG: gas chromatograph, FC: flow controller, ING: injection, TCD: thermal conductivity detector). Lower part: typical chromatographic response peaks.

oven where the temperature could be controlled within ±1 K. Prior to the experimental runs, the packed column was left at 393 K for 1h and then at 303 K under carrier gas flowing. The duration time of this second step was checked with the gas chromatograph until stabilization of the detected signal (baseline). Then, the tracer gas was injected in a pulse mode into the carrier gas stream using a six-port valve equipped with a sample loop of volume 0.1 ml. The response was detected at the column outlet by the TCD. The system was built and organized in such a way as to minimize the experimental errors caused by long gas lines and delayed response by the recorder. The mV signal of the detector was amplifier and recorded continually by the computer system which could collect more than 120 data points per min. All measurements were performed at 303 K and 99 kPa with a carrier gas flow varying between 5 and 45 $cm^3\,min^{-1}$. Each set of measurements was repeated no less than five times. Carrier gas flow rates were measured by a suitable flow meter.

3. Methodology

The moments of peaks (μ_1, μ_2'), appearing at the column outlet after injection of a square wave pulse of a tracer gas for a duration t_0 are related to the following parameters: The Henry law constant K and the intraparticle effective diffusivity D_{eff}.

The fist moment μ_1 and the second central moment μ_2' are given by [3]:

$$\mu_1 = \frac{L\varepsilon_b}{u}(1+\xi_0) + \frac{t_0}{2} \tag{1}$$

$$\mu_2' = \frac{2L\varepsilon_b}{u}(\xi_d + \xi_f + \xi_M) + \frac{t_0^2}{12} \tag{2}$$

where L is the column length (cm), ε_b the porosity of bed, u the carrier gas velocity ($cm^2\,s^{-1}$) and t_0 the injection time of the trace gas (s).

For rapid adsorption (i.e. linear adsorption equilibrium) of the tracer and negligible external mass transfer resistance the following relationships hold [7]

$$\xi_0 = \frac{(1-\varepsilon_b)\varepsilon}{\varepsilon_b}\left(1 + \frac{(1-\varepsilon)K}{\varepsilon}\right) \tag{3}$$

$$\xi_d = \frac{D_{ax}}{\varepsilon_b}(1+\xi_0)^2\left(\frac{\varepsilon_b}{u}\right)^2 \tag{4}$$

$$\xi_f = \frac{(1-\varepsilon_b)\varepsilon}{\varepsilon_b}\left(1 + \frac{(1-\varepsilon)K}{\varepsilon}\right)^2 \frac{R\varepsilon}{\gamma k_f} \tag{5}$$

$$\xi_M = \frac{(1-\varepsilon_b)\varepsilon}{\varepsilon_b}\left(1 + \frac{(1-\varepsilon)K}{\varepsilon}\right)^2 \frac{R^2}{\gamma(\gamma+2)D_{eff}} \tag{6}$$

where ε is the porosity of the particle arrangement/collection, K the Henry's law constant, R the mean radius of particle (cm), k_f is the external mass transfer coefficient ($cm\,s^{-1}$) and γ the particle shape factor (for spherical particles $\gamma = 3$).

The parameters ξ_o, ξ_d, ξ_f and ξ_M characterize the contribution of the adsorption resistance, the axial dispersion, the external mass transfer resistance and the intraparticle diffusion resistance respectively. The contribution of these parameters is additive and this advantage is used for the determination of adsorption factors and the diffusion coefficients.

The moments μ_1, μ_2' were calculated from the detector signal $H(t)$ by using the Simpson formula according the definition:

$$\mu_1 = \frac{\int_0^\infty tH(t)\,dt}{\int_0^\infty H(t)\,dt} \tag{7}$$

$$\mu_2' = \frac{\int_0^\infty (t-\mu_1)^2 H(t)\,dt}{\int_0^\infty H(t)\,dt} \tag{8}$$

3.1. Determination of parameters

The Henry law constant K is obtained easily by linear regression of the differences of the first moments (Eq. (1)) for adsorption runs with the tracer gas ($K \neq 0$) and runs with carrier gas ($K = 0$) versus the parameter ($\varepsilon_b L/u$).

$$\frac{\mu_1 - (\mu_1)_0}{((1-\varepsilon_b)(1-\varepsilon)/\varepsilon_b)} = K\frac{\varepsilon_b L}{u} \tag{9}$$

According to Eq. (9) the first term of this relationship is correlated linearly with the ($\varepsilon_b L/u$) and thus K is obtained from the slope of the corresponding line [3].

The effective diffusivities D_{eff} of the porous solids can be obtained from the second central (μ_2') moments. It is however, more convenient to use the so-called *chromatographic height equivalent to a theoretical plate*, HEPT, defined as

$$\text{HEPT} = \frac{\mu_2' L}{(\mu_1)^2} = 2\left(\frac{D_{ax}}{u} + \frac{(\xi_M + \xi_f)}{(1+\xi_0)^2}\left(\frac{u}{\varepsilon_b}\right)\right) \quad (10)$$

The contribution of axial dispersion D_{ax} becomes important when the flow velocity of the carrier gas is low. On the contrary, the contribution of the external mass transfer resistance ξ_f and the intraparticle diffusion resistance ξ_M are important when the flow velocity is high [3,4]. Based on the above assumptions, at higher velocities the axial dispersion resistance could be ignored without introducing any important error. According to Eq. (10), a linear relationship exists between the $(\mu_2' L/\mu_1^2)$ function on the left hand side and u. Then the parameters ξ_f and ξ_M are obtained from the slope of this line. However, the same slope corresponds to infinite flow velocity, where the contribution of external mass transfer resistance ξ_f is negligible. Thus, from the slope the parameter ξ_M is found from which the effective diffusivity D_{eff} is calculated according to Eq. (6).

The effective diffusivity D_{eff} is related to the composite diffusivity D_C by the expression:

$$\frac{D_p}{D_C} = \frac{\varepsilon}{\tau} \quad (11)$$

where τ is the tortuosity factor.

For diffusion of gases in porous solids, with very fine pores and for low concentration of diffused component within the particles, the Knudsen diffusion is significant. Neglecting the composition effect and at constant pressure, D_C is given by [18]:

$$D_C = \int_0^\infty \left(\frac{1}{D_{AB}} + \frac{1}{D_{K(r_p)}}\right)^{-1} f(r_p)\,dr_p \quad (12)$$

where D_{AB} is the binary bulk diffusivity for the gas mixture A, B, $D_{K(r_p)}$ is the Knudsen diffusivity in a pore of radius r_p and $f(r_p)$ is the pore size density function.

The Knudsen diffusivity in a pore of radius r_p and length l_p ($l_p \gg r_p$), is defined as [19]:

$$D_{K(r_p)} = 9700\, r_p \sqrt{\frac{T}{M}} \quad (13)$$

where the $D_{K(r_p)}$ is given in $cm^2\,s^{-1}$, T the temperature in Kelvin and M the molecular weight of diffused component ($g\,mol^{-1}$).

4. Results and discussion

The N_2 adsorption–desorption isotherms are shown in Fig. 1 for the hybrid organic–inorganic SiO_2-X solids. In the same Fig. 2, the pore size distributions (PSD) are shown, calculated according to the BJH method.

Table 1
Specific surface areas S_p, specific pore volumes V_p, mean pore diameter $\bar{D}_p$ of the PSD (see Fig. 1) and porosity ε for the SiO_2-X solids

Sample	S_p (BET) ($m^2\,g^{-1}$)	V_p (at $P/P_0 = 0.99$) ($cm^3\,g^{-1}$)	$\bar{D}_p$ (nm)	ε[a]
SiO_2	897	1.57	7.40	0.66
SiO_2–SiH	790	1.41	6.98	0.64
SiO_2–$SiCH_2OH$	776	1.34	6.90	0.63
SiO_2–$Si(CH_2)_3OH$	675	1.24	6.77	0.60
SiO_2–$Si(CH_2)_{11}CH_3$	584	1.13	6.75	0.59

[a] The porosity was calculated according the relation $V_p\rho_s(1 + V_p\rho_s)$ (where ρ_s is the effective specific density of the bulk solid equal to $2.5\,g\,cm^{-3}$).

In Table 1 the specific surface areas S_P ($m^2\,g^{-1}$) calculated according to the BET method and the specific pore volume V_P ($cm^3\,g^{-1}$) calculated from the total nitrogen volume adsorbed, are tabulated. In the same table the mean hydraulic pore diameter $\bar{D}_p = 4V_p/S_p$ of the pore size distribution and the porosity ε for all the SiO_2-X solids is shown. The initial porosity of the parent SiO_2 sample is blocked by the functionalization with the groups of increasing size, ≡Si–H, ≡Si–CH_2OH, ≡Si–$(CH_2)_3OH$ and ≡Si–$(CH_2)_{11}CH_3$. As expected this procedure results in a gradual drop of S_p (from 897 to 584 $m^2\,g^{-1}$) and V_p (from 1.57 to 1.13 $cm^3 g^{-1}$) values (Table 1). The mean hydraulic pore diameter $\bar{D}_p = 4V_p/S_p$ also decreases (from 7.40 to 6.77 nm). Those results are certainly due to the gradual blocking of pores by the functional groups. We mention that in Fig. 2 the SiO_2 samples functionalized with the longer groups depict larger pore size. This must be attributed to the fact the functionalization blocks preferably the smaller pores and as a result there remain the larger ones in the PSD which is moved to increase values.

As far as the diffusion parameters concern, calculation of the Henry's law constant K from the experimental first moments is straightforward according to Eq. (9). The lines representing the least square approximation of the data according to this equation for the examined SiO_2-X solids are shown in Fig. 3. The results obtained, i.e. the Henry law constant K as well as the correlation factor R_{sq} of the linear regression, are summarized in Table 2. The R_{sq} factor indicates very good linear fitting of the experimental data. The low values of K in Table 2 show that the adsorption of He on the porous surface for all the solids is weak [3].

Table 2
Henry law constant of tracing He

Sample	Correlation coefficient, R_{sq}	K[a]
SiO_2	0.9926	42.65
SiO_2–H	0.9983	41.98
SiO_2–CH_2OH	0.9789	41.52
SiO_2–$(CH_2)_3OH$	0.9982	38.30
SiO_2–$(CH_2)_{11}CH_3$	0.9974	41.97

[a] The calculations were estimated with porosity of the solids particle bed equal to $\varepsilon_b = 0.3$.

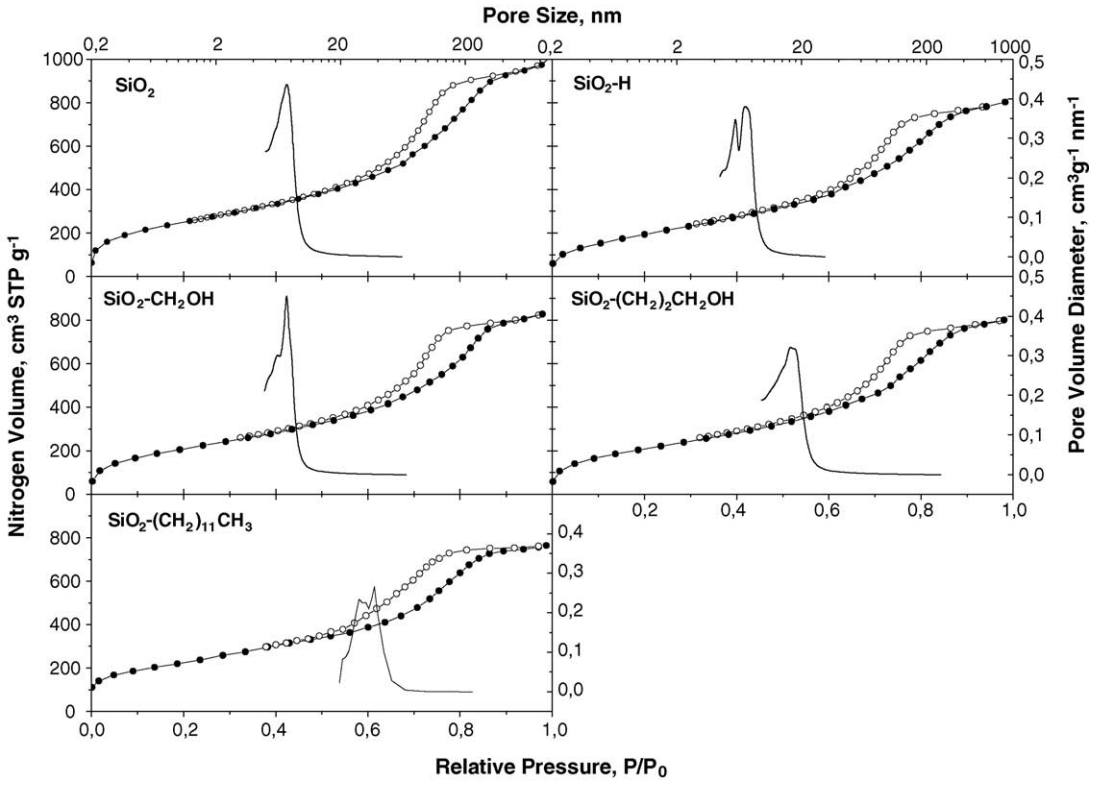

Fig. 2. N_2 adsorption–desorption isotherms and the corresponding PSD according to the BJH method for the hybrid organic–inorganic SiO_2-X materials.

The linear regressions of HEPT for different velocities u are shown in Fig. 4. The lines represent the least square approximation of the data according to Eq. (10). The results obtained are given also in Table 3, representing the slope, the intercept and the correlation factor R_{sq} of the linear regression as well as the effective diffusivity D_{eff} of the porous solids. The intercepts of the lines are not exactly equal to 0, but show small deviations which indicate only slight error incurred in the experimentation. In the same table, the composite diffusivity D_C and the tortuosity factors τ, estimated according to Eqs. (12) and (11) respectively, are cited. The results in Table 3 clearly indicate that as the length of carbon chain of the immobilized organic groups increases, the value of the effective diffusivity D_{eff} decreases roughly from 2.2 to 1.3×10^{-3} cm^2 s^{-1}, as actually expected. This effect is due to the gradual blocking of the pores with the functional

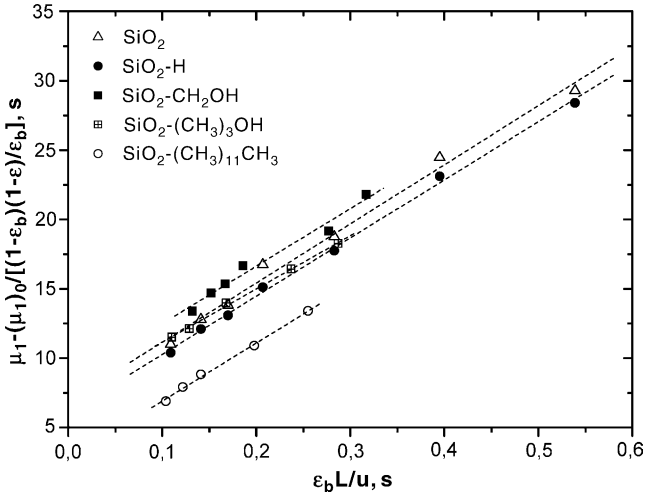

Fig. 3. Linear regression of $\mu_1 - (\mu_1)_0/[(1-\varepsilon_b)(1-\varepsilon_b)/\varepsilon]$ as a function of $(\varepsilon_b L/u)$ for the hybrid organic–inorganic SiO_2-X materials.

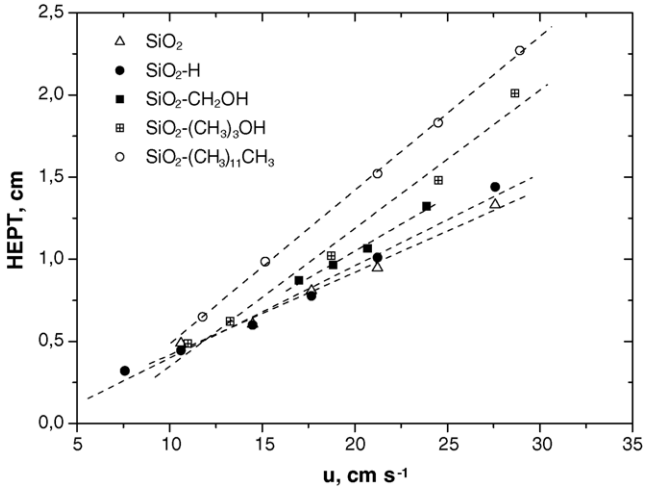

Fig. 4. Height equivalent to a theoretical plate (HEPT) vs. the carrier-gas velocity.

Table 3
Diffusion coefficients evaluated from the first and the second central moments as well as the corresponding tortuosity values

Sample	D_{eff}[a] (10^{-3} cm^2 s^{-1})	Slope	Intercept	Correlation coefficient, R_{sq}	D_C[b] (10^{-2} cm^2 s^{-1})	τ
SiO_2	2.176	0.0502	−0.0005	0.9883	2.988	9.10
SiO_2–H	2.011	0.0561	−0.0016	0.9858	2.896	9.22
SiO_2–CH_2OH	1.762	0.0655	−0.0026	0.9859	2.780	9.88
SiO_2–$(CH_2)_3OH$	1.412	0.0841	−0.0049	0.9855	2.530	10.89
SiO_2–$(CH_2)_{11}CH_3$	1.306	0.0937	−0.0045	0.9996	2.445	11.12

[a] The calculations were with bed porosity equal to $\varepsilon_b = 0.3$ and mean radius of particles equal to $R = 2$ μm.
[b] The binary bulk diffusivity was $D_{He–N_2} = 0.730$ cm^2 s^{-1} at $T = 303$ K [20].

groups, which restrict the diffusion. Actually D_{eff} shows a dependence on the mean pore diameter D_p of the silica samples as shown in Fig. 5. It can be seen that D_{eff} initially increases very fast as D_p increases from 6.7 to 7.0, while thereafter this influence becomes more weak and almost ceases. This behavior should correspond to the transition from the Knudsen-type diffusion to the bulk-type diffusion (see Eqs. (12) and (13)) as expected in this range of D_p [3,19].

In Table 3, we observe that the tortuosity τ values increase gradually with the carbon length of functional group from $\tau = 9.1$ at X = Ø to $\tau = 11.1$ at X = ≡Si–$(CH_2)_{11}CH_3$. The increase of the τ values with the pore blocking can be intuitively understood as follows: The increase of immobilized carbon chains, blocks some of the paths, presumably those corresponding to smaller pores. The removal of those fine by-passes has as a result that the remaining of the routes consisted of more lengthy larger by-passes. In such an environment the diffused molecules have less possibilities for easy access between any two random points of the network. Finally, we notice that some time ago Sands, Kim and Bass [21] carried out a detailed study of porous silicas functionalized with N-alky-dimethyl-chlorosilanes $C_nH_{2n+1}(CH_3)_2SiCl$ with n–1, 4, 8 and 18. Those materials were used in HPLC for small molecules like phenols, acetophenone, etc. as well as protein molecules like ribonuclease insulin, lysozyme, etc. They found opposite effects of pore diameter D_p and pore volume V_p on the small molecules (negative effects) compared to large proteinic species (positive effects). These effects should be related to the resolution of apparent D_{eff} in each case which were not directly measured. Nevertheless such studies show that the manipulation of the surface by various functional groups can have varying effects on the D_{eff} of small or large species, a fact which can be attributed not only to the chemical nature as in 21 but also to geometrical and spatial reason as in the present study.

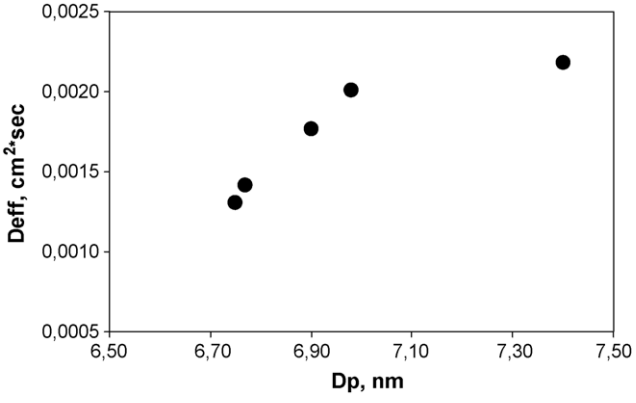

Fig. 5. Dependence of the D_{eff} (cm^2 s) on the mean pore diameter D_p (nm) of the silicas.

5. Conclusions

A linearization method for determining effective diffusivity and Henry law constants of gas in porous solids was developed. The diffusion parameters of binary gas mixture He (tracer gas)–N_2 (carrier gas) have been estimated for five hybrid organic–inorganic SiO_2-X porous solids which suffered gradual functionalization with functional groups X of increasing length (X = Ø, ≡Si–H, ≡Si–CH_2OH, ≡Si–$(CH_2)_3OH$, ≡Si–$(CH_2)_{11}CH_3$). The results of this work indicate that the effective diffusivity of porous network drops markedly from 2.2 to 1.3×10^{-3} cm^2 s^{-1} as the initial porosity of the parent SiO_2 sample is blocked by the functionalization with functional groups of increasing size, ≡Si–H, ≡Si–CH_2OH, ≡Si–$(CH_2)_3OH$ and ≡Si–$(CH_2)_{11}CH_3$. Also, the tortuosity factor increases from $\tau = 9.1$ at X = Ø to $\tau = 11.1$ at X = ≡Si–$(CH_2)_{11}CH_3$ and is correlated proportionally to the pore blocking effects and the percolation phenomena into the pore network.

6. Nomenclature

$\bar{D}_p$	mean pore diameter (nm)
D_{AB}	binary bulk diffusivity of pair A–B (cm^2 s^{-1})
D_{ax}	axial dispersion coefficient (cm^2 s^{-1})
D_C	composite diffusivity (cm^2 s^{-1})
D_{eff}	effective diffusivity (cm^2 s^{-1})
$D_{K(r_p)}$	Knudsen diffusivity in circular capillary of radius r_p (cm^2 s^{-1})
$f(r_p)$	pore size density function
$H(t)$	detector signal
HEPT	height equivalent to a theoretical plate (cm)
K	Henry law constant
L	column length (cm)
l_p	pore length (cm)
M	molecular weight (g mol^{-1})
P/P_0	relative pressure

R	mean radius of particle (cm)
r_p	pore radius (cm)
R_{sq}	correlation factor of linear regression
S_p	specific surface area ($m^2\,g^{-1}$)
t	time
T	temperature (K)
t_0	injection time of trace gas (s)
u	linear flow velocity of carrier gas ($cm\,s^{-1}$)
V_p	specific pore volume ($cm^3\,g^{-1}$)

Greek symbols

γ	particle shape factor
ε	particle porosity
ε_b	bed porosity
μ'_2	second central moment (s^2)
μ_1	first moment (s)
ξ_o	adsorption resistance
ξ_d	axial dispersion resistance
ξ_f	external mass transfer resistance
ξ_M	intraparticle diffusion resistance
ρ_s	bulk density of particle ($g\,cm^{-3}$)
τ	tortuosity factor

Acknowledgements

We acknowledge financial support from EU under the project GROWTH–INORGPORE (G5RD-CT-2000-00317) and from PYTHAGORAS project of the Ministry of Education.

References

[1] W. Henry, J.R. Haynes, Catal. Rev. Sci. Eng. 30 (1988) 563.
[2] J. Kärger, D.M. Ruthven, Diffusion in Zeolites and Other Microporous Solids, Wiley, New York, 1992.
[3] D.D. Do, Adsorption Analysis: Equilibria and Kinetics, Series on Chemical Engineering, vol. 2, Imperial College Press, 1998.
[4] (a) A.S. Chiang, A.G. Dixon, Y.H. Ma, Chem. Eng. Sci. 39 (1984) 1451;
(b) A.S. Chiang, A.G. Dixon, Y.H. Ma, Chem. Eng. Sci. 39 (1984) 1461.
[5] A.G. Dixon, Y.H. Ma, Chem. Eng. Sci. 43 (1988) 1297.
[6] H.W. Haynes, AIChE J. 32 (1986) 1750.
[7] G.S. Yu, J. Yu, Z. Yu, Chem. Eng. J. 78 (2000) 141.
[8] H. Boniface, D.M. Ruthven, Chem. Eng. Sci. 40 (1985) 1401.
[9] M. Kubin, Collect. Czech. Chem. Commun. 30 (1965) 2900.
[10] E. Kučera, J. Chromatogr. 14 (1965) 237.
[11] M. Suzuki, J.M. Smith, Adv. Chromatogr. 13 (1975) 213.
[12] N. Wakao, S. Kaguei, J.M. Smith, Ind. Eng. Chem. Fundam. 19 (1980) 363.
[13] D.S. Scott, W. Lee, J. Papa, Chem. Eng. Sci. 29 (1974) 2155.
[14] J. Crank, The Mathematics of Diffusion, Clarendon Press, Oxford, 1975.
[15] A. Baiker, M. New, W. Richarz, Chem. Eng. Sci. 37 (1982) 643.
[16] C.C. Fu, M.S.P. Ramesh, H.W. Haynes, AIChE J. 32 (1986) 1848.
[17] P.J. Pomonis, G.S. Armatas, Langmuir 20 (2004) 6719.
[18] B.C. Zhu, Inorganic Chemical Reaction Engineering, Chemical Industry Press, Beijing, 1981.
[19] C.N. Satterfield, Mass Transfer in Heterogeneous Catalysis, M.I.T. Press, Cambridge, 1970, p. 41.
[20] R.C. Reid, T.K. Sherwood, The Properties of Gases and Liquids, second ed., McGraw-Hill, New York, 1966 (Series in Chemical Engineering).
[21] B.W. Sands, Y.S. Kim, J.L. Bass, J. Chromatogr. 360 (1986) 353.